Protein Science (1994), *3*:628-637. Cambridge University Press. Printed in the USA.

Distribution of distances between the tryptophan and the N-terminal residue of melittin in its complex with calmodulin, troponin C, and phospholipids

JOSEPH R. LAKOWICZ,[1] IGNACY GRYCZYNSKI,[1] GABOR LACZKO,[1]
WIESLAW WICZK,[1] AND MICHAEL L. JOHNSON[2]

[1] Department of Biological Chemistry, Center for Fluorescence Spectroscopy, School of Medicine, University of Maryland, Baltimore, Maryland 21201
[2] Department of Pharmacology, Jordan Hall, Box 448, University of Virginia, Charlottesville, Virginia 22908

(RECEIVED July 20, 1993; ACCEPTED February 2, 1994)

Abstract

We used frequency-domain measurements of fluorescence resonance energy transfer to measure the distribution of distances between Trp-19 of melittin and a 1-dimethylamino-5-sulfonylnaphthalene (dansyl) residue on the N-terminal-α-amino group. Distance distributions were obtained for melittin free in solution and when complexed with calmodulin (CaM), troponin C (TnC), or palmitoyloleoyl-L-α-phosphatidylcholine (POPC) vesicles. A wide range of donor (Trp-19)-to-acceptor (dansyl) distances was found for free melittin, which is consistent with that expected for the random coil state, characterized by a Gaussian width (full width at half maxima) of 28.2 Å. In contrast, narrow distance distributions were found for melittin complexed with CaM, 8.2 Å, or with POPC vesicles, 4.9 Å. A somewhat wider distribution was found for the melittin complex with TnC, 12.8 Å, suggesting the presence of heterogeneity in the mode of binding between melittin and TnC. For all the complexes the mean Trp-19 to dansyl distance was near 20 Å. This value is somewhat smaller than expected for the free α-helical state of melittin, suggesting that binding with CaM or TnC results in a modest decrease in the length of the melittin molecule.

Keywords: calmodulin; distance distributions; fluorescence spectroscopy; frequency-domain fluorescence; melittin; protein conformation; protein folding; resonance energy transfer; troponin C

Melittin is a 26-amino acid amphipathic peptide from bee venom that is known to adopt a range of conformational states depending upon its concentration and the ionic strength and chemical composition of the solution. At low ionic strengths melittin exists as a random coil monomer (Faucon et al., 1979; Talbot et al., 1979; Goto & Hagihara, 1992), presumably due to electrostatic repulsion between the positively charged amino acid side chains. As the ionic strength is increased, melittin forms tetramers in which the monomeric units are in the α-helical state. The self-association appears to be stabilized by hydrophobic interactions between the nonpolar surfaces of the monomer that are created upon formation of the helices. Melittin is also known to adopt an α-helical state in methanol/water mixtures (Bazzo et al., 1988). The amphipathic properties of melittin result in its interaction with a variety of biomolecules. Melittin is known to form complexes with calmodulin in the presence of Ca^{2+} (Comte et al., 1983; Maulet & Cox, 1983; Steiner et al., 1986), with troponin C (Steiner & Norris, 1987; Strynadka & James, 1990), and upon interaction with detergents and phospholipids (Dawson et al., 1978; Strom et al., 1978; Drake & Hider, 1979; Knoppel et al., 1979; Lavialle et al., 1982; Stanislawski & Rüterjans, 1987; Dempsey et al., 1989; Kuchina & Seelig, 1989; Beschiaschvili & Seelig, 1990). In the present report we describe the conformational changes of melittin upon complexation with proteins and membranes.

We used fluorescence resonance energy transfer to examine the conformation changes of melittin upon complex formation. The energy donor was the Trp residue at position 19, and the acceptor was a dansyl residue on the N-terminal α-amino group. FRET has been widely used to measure distances between discrete sites on macromolecules (Stryer & Haugland, 1967; Cheung, 1991). This method has traditionally been used in cases where the protein adopts a single conformation. However, there are

Reprint requests to: Joseph R. Lakowicz, Department of Biological Chemistry, University of Maryland School of Medicine, 108 N. Greene Street, Baltimore, Maryland 21201; e-mail: jf@sg.ab.umd.edu.

Abbreviations: CaM, calmodulin; DNS or dansyl, 1-dimethylamino-5-sulfonylnaphthalene; FRET, fluorescence resonance energy transfer; Mops, 3-(*N*-morpholino)propanesulfonic acid; POPC, palmitoyloleoyl-L-α-phosphatidylcholine; TnC, troponin C.

many situations in which a single conformation does not exist, such as for the random-coil state of proteins. In this case, a measure of the energy transfer efficiency does not reveal the underlying distance distribution. In the present case we expect the random-coil state of melittin to exist in a range of conformations, and one cannot predict a priori that a single unique conformation exists upon complexation with proteins or lipids.

Additional information about conformation distributions is available from time-resolved studies of energy transfer. More specifically, the data can be used to recover distributions of distances between donor and acceptor (Lakowicz et al., 1987b, 1988a; Cheung, 1991). This information is available because the distribution of donor-to-acceptor distance results in a distribution of energy transfer rates, which in turn results in a complex intensity decay of the donor. Such measurements may be performed using time-domain (Hedstrom et al., 1990; Beals et al., 1991; Kaschke et al., 1991; Prochazka et al., 1992) or frequency-domain data (Lakowicz et al., 1988b, 1990). We note that the concept of distance distribution analysis was pioneered by the work of Steinberg, Haas, and co-workers (Haas et al., 1975; Amir & Haas, 1986), in which the time-dependent decay of donor fluorescence was used to recover the donor-to-acceptor distance distribution. Our approach is similar, except for the use of the frequency-domain method to recover the donor decay kinetics (Gratton & Limkeman, 1983; Lakowicz & Maliwal, 1985; Lakowicz et al., 1986a).

Melittin provides an ideal model for such studies because it possesses a single Trp residue at position 19 that can serve as an energy donor for the calculation of point-to-point distances. CaM and TnC both lack Trp residues, and the single Trp residue of melittin can be excited without excitation of the Tyr residues in CaM or TnC. The distance distribution method requires that both the donor and acceptor be present at single sites on the macromolecules, and that a single acceptor be present on all of the donor- and A-labeled molecules. Such specific and complete labeling could be a formidable problem for melittin because of the number of Lys residues and their similar reactivity with amino-reactive chromophores. To circumvent the potential problem of multiple-labeled sites, melittin was synthesized de novo and labeled at the α-NH_2-terminal Gly with a dansyl moiety (Weaver et al., 1989). The Förster distance for Trp-to-dansyl transfer is known to be near 20 Å (Lakowicz et al., 1990, 1994), which seemed appropriate for sites separated by 18 amino acid residues.

At present, X-ray crystal structures are known for melittin (Terwilliger & Eisenberg, 1982; Terwilliger et al., 1982), CaM (Babu et al., 1985, 1988; Kretsinger et al., 1985), and for TnC (Herzberg & James, 1985, 1988; Sundaralingam et al., 1985; Satyshur et al., 1988). The crystal structures of the melittin–CaM or melittin–TnC complexes have not been reported, but there have been reports of structures of amphipathic peptides bound to CaM (Strynadka & James, 1990; Ikura et al., 1992; Meador et al., 1992, 1993; Precheur et al., 1992). To the extent possible, our results are compared with these published structures.

Results

Characterization of melittin–protein complexes

In the presence of Ca^{2+} the binding between melittin and CaM or melittin and TnC is expected to be complete under our experimental conditions. This was confirmed by measurements of the steady-state Trp anisotropy of melittin with increasing amounts of CaM or TnC (Fig. 1). The anisotropy becomes constant at a 1:1 mol ratio of protein to melittin. The same results were obtained for dansyl-melittin, which indicates that the presence of the N-terminal dansyl moiety does not interfere with the binding. The consistently larger steady-state anisotropy observed for dansyl-melittin as compared with melittin is the result of shortening the mean Trp decay time by energy transfer. All further experiments were performed using the 1.2-to-1.0 ratio of CaM or TnC to melittin.

In our calculation of the distance distributions, we assume that energy transfer occurs to a single acceptor. This assumption would be in error if the CaM molecule bound more than 1 melittin molecule, as reported by Follenius-Wund et al. (1987). In fact, casual analysis of Figure 1 suggests that the changes in anisotropy saturate near 0.6 equivalents of CaM, which could suggest binding of more than 1 melittin per CaM. The early apparent saturation in Figure 1 is the result of the higher relative intensity of melittin when bound to CaM (insert) at the observation wavelength of 340 nm. To evaluate further the possibility of the higher complexes, we used the reported values of the dissociation constants for melittin·CaM (Maulet & Cox, 1983; Milos et al., 1987), melittin·CaM_2 (Follenius-Wund et al., 1987) to calculate the concentration of these complexes in our solution with a 20% excess of CaM (Fig. 1). These solutions indicate that the 1-to-1 complex is in a 100–200-fold excess over

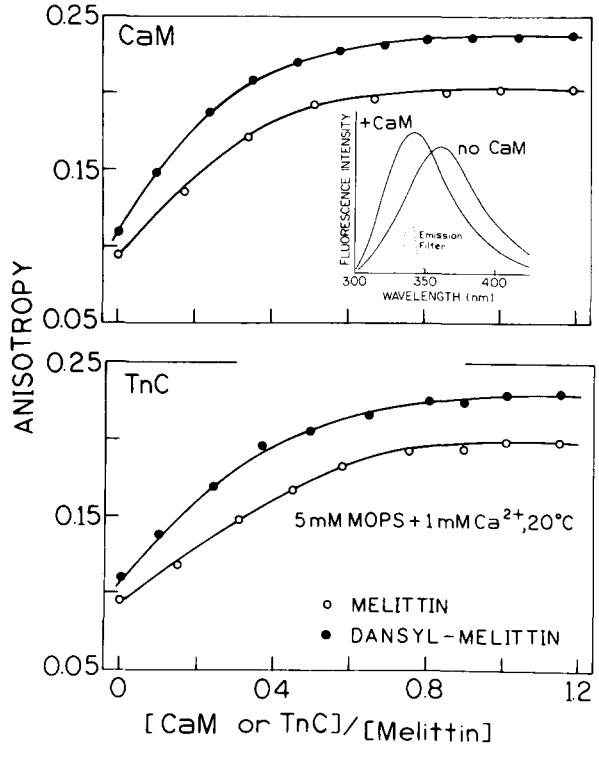

Fig. 1. Steady-state fluorescence anisotropy of melittin (O) and dansyl-melittin (●) as titrated with CaM (top) or TnC (bottom). The concentrations of melittin and dansyl-melittin were 2×10^{-5} M. The inset shows the emission spectra of melittin with and without CaM. The excitation was at 298 nm, and the emission was observed through a 340-nm, 10-nm-bandpass interference filter.

the 2-to-1 complex. Given that a second acceptor would result in additional energy transfer and a decreased contribution to the measured Trp emission, the 2-to-1 complexes, if present, cannot have a significant effect on the results.

The melittin-CaM complex was further characterized by its frequency-domain anisotropy decay (Fig. 2). The anisotropy decay shows a subnanosecond component that accounts for about 27% of the total anisotropy, which is typical of the anisotropy decays of globular proteins (Lakowicz et al., 1986a; Steiner, 1991). The dominant component of the anisotropy decay displays a rotational correlation time near 6 ns. For a 1-to-1 complex of melittin (MW 2,840) and CaM (MW 16,800), with a molecular weight of 19,640 Da, one expects a correlation time near 7 ns, assuming the complex is spherical with 10-20% hydration (Steiner, 1991). Similar correlation times were observed for the complexes between DNS-melittin, CaM, and TnC, indicating the dominant presence of a 1-to-1 complex (Table 1). It is possible that these apparent overall correlation times are shorter than the actual values due to the inevitable contribution of protein segmental motions to the data. In the absence of CaM or TnC, the anisotropy decay is dominated by a 0.17-ns component. The remainder of the anisotropy displays a correlation time of 1.7 ns. These correlation times are characteristic of substantial segmental motions in the largely random-coil state of melittin (Lakowicz et al., 1987a). The larger contribution of the shorter correlation time for monomeric melittin is the result of local motions of the Trp residue as well as diffusive motions of the peptide chain (Lakowicz et al., 1994). In the presence of CaM or TnC these typical motions of a random flexible polypeptide are damped, presumably due to loss of segmental and local side-chain motion in the complex (Maulet & Cox, 1983).

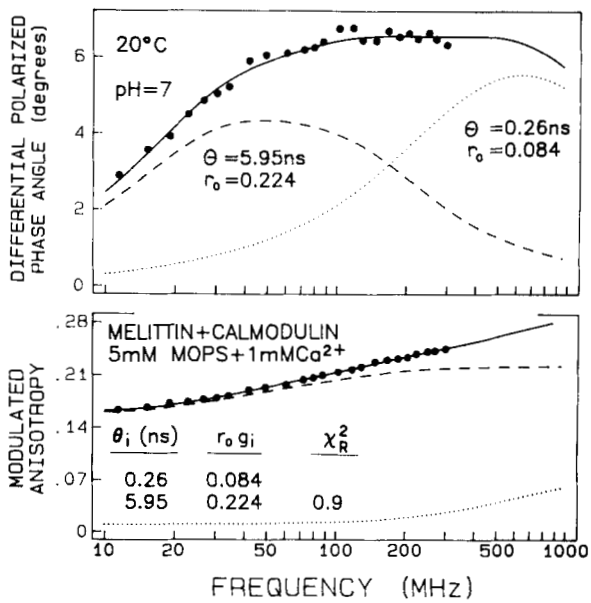

Fig. 2. Frequency-domain anisotropy decay of the melittin-CaM complex. The dashed and dotted lines indicate the separate contributions of the 2 correlation times to the data.

Emission spectra

Emission spectra of melittin and dansyl-melittin when complexed with CaM are shown in Figure 3. The Trp emission is centered at 355 nm, and the emission from the dansyl residue occurs near 485 nm. The presence of energy transfer is seen from the decrease in the Trp fluorescence intensity when the dansyl moiety is present. The efficiency of energy transfer is about 47%, which corresponds to an apparent distance of 21.4 Å for an R_0 value of 21 Å. Similar emission spectra were observed for the complex with TnC. The efficiency of energy transfer was 58%, resulting in an apparent distance of 19.6 Å for an R_0 value of 20.6 Å. It should be emphasized that these apparent distances are only meaningful if there is a single donor-to-acceptor distance.

Frequency-domain donor decays

The frequency responses of the Trp decays of melittin and dansyl-melittin are shown in Figure 4. The effect of energy transfer to the dansyl residue is seen from the shift in the frequency response toward higher frequencies. These results and the resulting distance distributions (below) are in agreement with those found previously for random-coil melittin in the absence of calcium (Lakowicz et al., 1990). This indicates that Ca^{2+} itself does not affect the conformational distribution of melittin under our experimental conditions, nor would it be expected to have an influence. Similar data for the melittin-CaM and for the melittin-TnC complexes are shown in Figure 5. In these cases, the extent of energy transfer is greater than in the absence of CaM, as can be seen by the somewhat larger shift in the frequency response. In all cases, the data are well fit by the triple-exponential model, shown as solid lines in Figures 4 and 5.

Table 1. *Tryptophan and dansyl anisotropy decays for melittin and melittin complexes*[a]

Sample	θ_j (ns)	$r_0 g_j$	χ^2_R 1[a]	2	3
Tryptophan fluorescence					
Melittin	0.17	0.193			
	1.73	0.126	14.1	0.9	0.9
Melittin + CaM	0.26	0.084			
	5.95	0.224	26.1	0.9	–
Melittin + TnC	0.37	0.107			
	6.10	0.205	54.8	1.0	–
Melittin + POPC	0.19	0.163			
	1.64	0.058			
	41.04	0.100	88.6	1.6	1.0
Dansyl fluorescence					
Dansyl-melittin	0.19	0.192			
	1.87	0.114	8.3	1.6	1.6
Dansyl-melittin + CaM	0.58	0.032			
	7.23	0.219			
	11.09	0.057	5.6	1.5	1.5
Dansyl-melittin + POPC	0.72	0.009			
	3.34	0.140			
	92.86	0.136	97.1	1.2	1.2

[a] Values of χ^2_R are shown for the 1, 2, and 3 correlation time fits. Anisotropy decay parameters are only shown for the accepted 2 or 3 correlation time model.

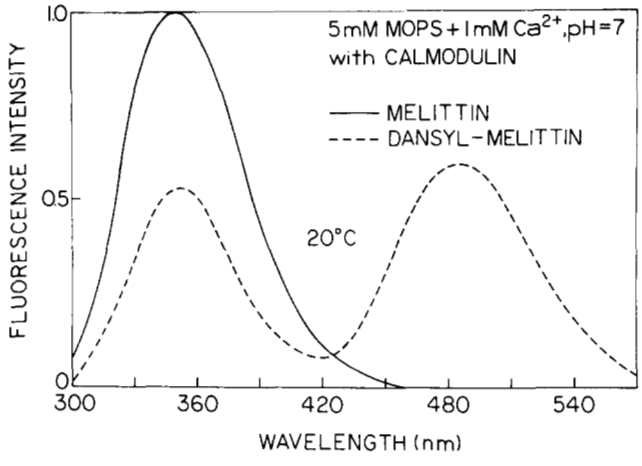

Fig. 3. Emission spectra of melittin and dansyl-melittin when complexed with CaM. The extent of energy transfer, as observed from the peak intensities of the donor, was 47%. Similar spectra were observed for dansyl-melittin with TnC or POPC, except that the extents of energy transfer were 58 and 41%, respectively.

The multiexponential analyses of melittin and dansyl-melittin are summarized in Tables 2 and 3, respectively. In all cases the Trp decays were strongly heterogeneous, with χ_R^2 values ranging from 340 to 1,000 for the single exponential fits. The double-exponential fits were also inadequate, yielding χ_R^2 values 3-7-fold larger than the acceptable triple-exponential fits. We recognize that these decays may not actually be a sum of exponentials, especially in the case of energy transfer to the acceptor at various distances. However, the decay parameters in Tables 2 and 3 represent the frequency-domain data to within the accuracy of the measurements and may be useful for future comparisons with time-resolved measurements or theoretical calculations of the conformational distributions of melittin.

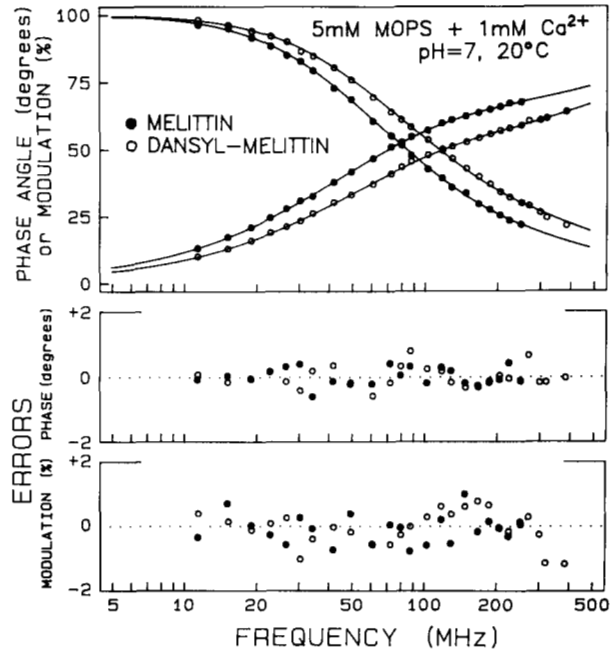

Fig. 4. Frequency response of the Trp intensity decay for melittin (●) and dansyl-melittin (○). The dots (●, ○) show the data and the solid lines show the best triple-exponential fits to the data. The lower panels show the deviations between the data and the best triple-exponential fits.

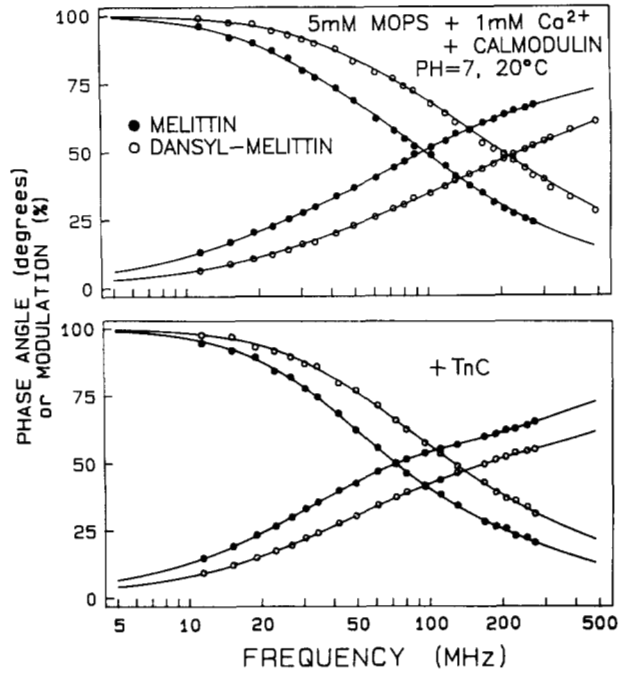

Fig. 5. Frequency response of the Trp intensity decay in melittin and dansyl-melittin when complexed with CaM (top) and with TnC (bottom). The solid lines show the best triple-exponential fits to the data.

Distance distribution analysis

The pairwise data for melittin and dansyl-melittin were analyzed to recover the distribution of donor-to-acceptor distances. One such analysis is shown in Figure 6 for dansyl-melittin in 5 mM Mops, which is expected to be present in the random-coil state. The data can be well fit by a wide distribution of donor-to-acceptor distances, with a mean ($\bar{r}$) and half-width (*hw*) of 16.3 and 28.0 Å, respectively (—). We attempted to force fit the data to a narrow *hw* of 1 Å. The attempt resulted in an unacceptable fit to the data (---), large and nonrandom deviations (lower panel, ○○○), and an unacceptable value for χ_R^2, 132.2. We conclude that, at low ionic strength, melittin exists in a range of conformations, resulting in a range of Trp-19 to N-α-amino dansyl distances. For this wide distribution part of the Gaussian occurs below a distance of zero. This simply indicates that the donor-to-acceptor distribution has significant probability at short distances. The distributions are normalized to the physically meaningful values above r_{min} (Equation 16).

Next we performed a distance-distribution analysis for the complex between dansyl-melittin and CaM (Fig. 7). In this case the frequency-domain data indicated a much narrower distribution, with $\bar{r}$ = 19.4 Å and *hw* = 8.2 Å. The 8-Å *hw* appears to be characteristic of the complex. This is shown by our inability to fit the data to either a wider (25 Å) or a narrower (1 Å) distribution. In both forced fits the data did not match the calculated curves and the χ_R^2 values increased 20-30-fold.

Table 2. *Multiexponential analyses of the melittin tryptophan intensity decays*

Conditions[a]	$\bar{\tau}$ (ns)[b]	τ_i (ns)	α_i	f_i	χ_R^2 1[c]	2	3
Melittin	4.02	0.41	0.375	0.069			
		2.95	0.530	0.697			
		5.54	0.095	0.234	341	3.7	1.4
Melittin + CaM	4.23	0.32	0.307	0.051			
		1.85	0.555	0.533			
		5.81	0.138	0.461	502	140	2.1
Melittin + TnC	4.88	0.60	0.522	0.138			
		3.46	0.335	0.510			
		5.61	0.143	0.352	907	3.2	0.8
Melittin + POPC	3.95	0.21	0.350	0.034			
		1.90	0.394	0.344			
		5.29	0.256	0.622	523	11.3	1.4

[a] All solutions were in 5 mM Mops, pH 7, 20 °C, also containing 1 mM Ca^{2+}.
[b] $\bar{\tau} = \Sigma_i f_i \tau_i$.
[c] The values of χ_R^2 are for the single- (1), double- (2), and triple- (3) exponential models.

The distance distributions for all the melittin complexes are shown in Figure 8 and summarized in Table 4. The mean distance was similar in the 2 complexed states (CaM or TnC), and a slightly longer distance for the complex with POPC, which are all thought to be α-helical. The narrowest and longest distribution was observed for melittin bound to POPC. This result may reflect a lack of constraint on the melittin conformation by the lipids. To be specific, in contrast to the proteins, the lipids do not have a defined distribution of charges and hydrophobic surfaces that can constrain the 3-dimensional conformations of melittin. It is interesting to note that a similar narrow distance distribution was observed for melittin in methanol (Lakowicz et al., 1990), which would also pose no steric restrictions on the conformation of melittin. The wider distribution observed for the melittin complexes with CaM or TnC may reflect distortions of the melittin structure to conform to the hydrophobic patch expressed by these proteins in the presence of Ca^{2+}. There may be some heterogeneity in the modes of binding between melittin and CaM or TnC to account for the heterogeneity in distances. However, $\bar{r}$ and *hw* are similar for the CaM and troponin complexes, which is expected based on the structural similarities of these proteins (Heidorn & Trewhella, 1988).

Table 3. *Multiexponential analysis of dansyl-melittin tryptophan intensity decays*

Conditions[a]	$\bar{\tau}$ (ns)[b]	τ_i (ns)	α_i	f_i	χ_R^2 1[c]	2	3
Dansyl-melittin (DM)	3.24	0.38	0.531	0.141			
		2.25	0.395	0.621			
		4.60	0.074	0.238	790	5.3	1.9
DM + CaM	2.25	0.30	0.526	0.180			
		1.14	0.398	0.516			
		3.53	0.076	0.304	629	12.8	3.1
DM + TnC	2.85	0.36	0.580	0.171			
		1.62	0.264	0.356			
		3.65	0.156	0.473	1005	6.5	2.1
DM + POPC	2.08	0.24	0.387	0.078			
		1.33	0.478	0.530			
		3.47	0.135	0.392	480	13.6	2.0

[a] All solutions were in 5 mM Mops, pH 7, 20 °C, also containing 1 mM Ca^{2+}.
[b] $\bar{\tau} = \Sigma_i f_i \tau_i$.
[c] The values of χ_R^2 are for the single- (1), double- (2), and triple- (3) exponential fits.

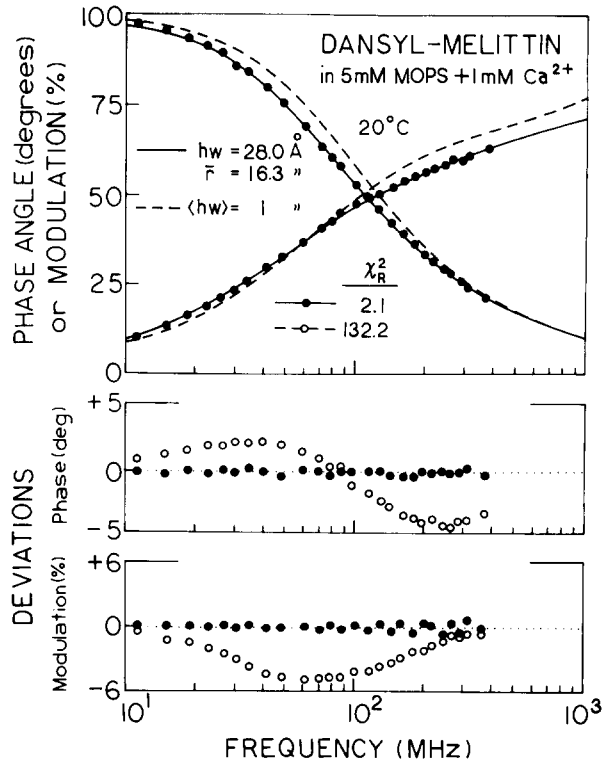

Fig. 6. Distance-distribution analysis of dansyl-melittin with 1 mM Ca^{2+}. The solid line represents the best fit to the data (●). The dashed line represents the best fit with the *hw* held constant at 1 Å. The lower panels show the deviations with *hw* = 28.0 Å (●) and 1 Å (○).

Finally, we considered the uncertainties in the values of $\bar{r}$ and *hw* recovered from our data. These uncertainties were first estimated from the least-squares analysis, with consideration of correlation between the parameters (Johnson, 1983). This analysis (Table 4) indicates little uncertainty in either $\bar{r}$ or *hw*, with the range being about ±0.3 Å for each parameter. A second estimation of the uncertainties was performed by examining the χ_R^2 surface for each parameter (Fig. 9). The range of parameter values consistent with the data is given by those that occur below the dashed lines. This analysis indicates that $\bar{r}$ for the 3 α-helical states are within experimental error of each other, whereas $\bar{r}$ for the random-coil state is distinct. Interestingly, the *hw*'s of the 3 α-helical states are distinct from each other, indicating that our experimental resolution is adequate to detect the conformational differences between these states.

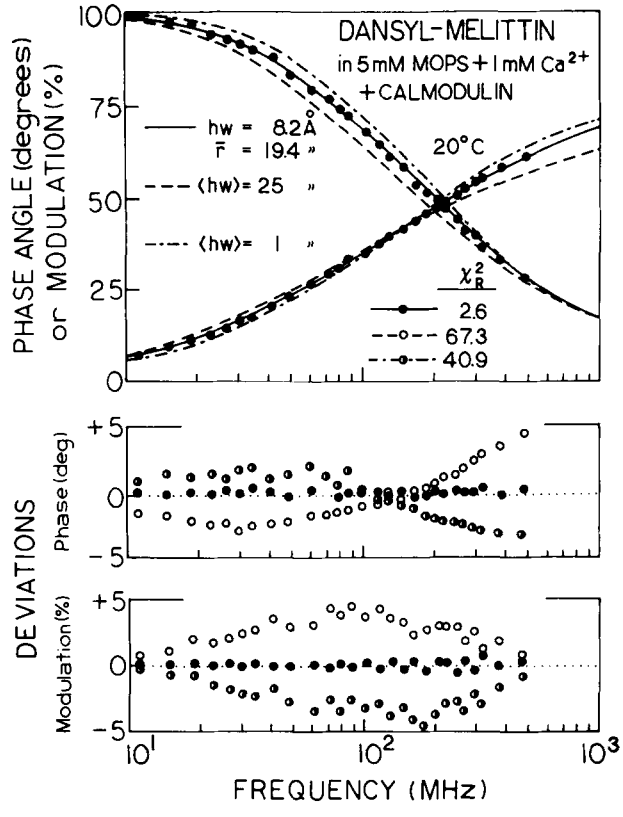

Fig. 7. Distance-distribution analysis of the dansyl-melittin-CaM complex. The solid line represents the best fit of the Gaussian distance model to the experimental data (●). The broken lines show the best fit when the *hw* was held constant at 20.1 Å (---) or 9 Å (-·-·-). The lower panels show the deviations with *hw* = 8.2 Å (●), 20.1 Å (◑), and 1.0 Å (○).

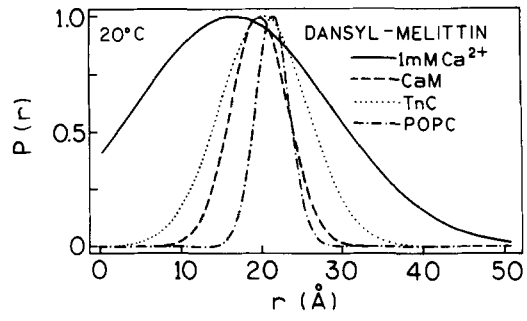

Fig. 8. Distribution of Trp-to-dansyl distances in melittin and its complexes with CaM, TnC, or POPC.

Discussion

It is known that distance measurements can be uncertain due to the unknown value of the orientation factor κ^2 (Dale & Eisinger, 1975, 1979). In the present case we observed substantial motional freedom of both the donor and acceptor (Table 1). In such cases the range of κ^2 values are rather limited (Lakowicz et al., 1988b; Cheung, 1991). Additionally, the extent of motional freedom is similar in the various melittin complexes. Hence, the relative values of the distance-distribution parameters are unlikely to be affected by the orientation factor.

It is interesting to note that the mean donor-to-acceptor distances in the melittin-CaM and melittin-TnC complex (≈20 Å) are smaller than that observed for the α-helical state of melittin in a methanol-water mixture (≈25 Å; Lakowicz et al., 1990) or when bound to POPC (≈21 Å). This suggests that complexation with CaM or TnC results in a structural rearrangement that brings together the Trp-19 and N-terminal residues of melittin. This experimental result is consistent with modeling studies of the interaction of CaM and TnC with amphipathic helices (Strynadka & James, 1990). In order to position melittin onto CaM it was necessary to bend the N-terminal segment of melittin by 180° around its helix axis. These steric interactions and bending of the CaM or TnC (Vorherr et al., 1992) may be the origin of the apparently shortened length of the melittin molecules, relative to unrestrained melittin in methanol. It is also interesting to notice that the mean donor-to-acceptor distance for melittin bound to POPC vesicles (≈21 Å) is also smaller than in the methanol-water mixture. One possible explanation of this shorter distance is bending of the helix upon binding to lipids, or shielding of electrostatic repulsion between like charges on melittin when present at the highly charged lipid-water interface. Bending of the α-helix has been suggested for a synthetic peptide analogue of the CaM-binding domain myosin light chain kinase when bound to CaM (Roth et al., 1991). Alternatively, the highly charged melittin molecule may be subjected to less electrostatic repulsion when present at the highly charged lipid-water interface.

In summary, time-resolved energy transfer studies of melittin have provided detailed information concerning its conformational variability when bound to proteins and lipids.

Theory

The theory of energy transfer in the presence of distance distributions has been described elsewhere in detail (Lakowicz et al., 1987b, 1988a, 1988b) and is briefly summarized below. We assume that the probability that a donor-acceptor pair are separated by a distance r is given by a Gaussian:

Table 4. *Distance-distribution parameters for dansyl-melittin*

Conditions[a]	R_0 (Å)	$\bar{r}$ (Å)	*hw* (Å)	χ^2_R
Dansyl-melittin (DM)	19.6	16.2 ± 0.56	28.2 ± 1.00	2.2
		21.7	⟨1⟩[b]	132.2
		17.8	⟨25⟩	2.4
DM + CaM	21.0	19.4 ± 0.04	8.2 + 0.14	2.6
		20.1	⟨1⟩	40.9
		9.0	⟨25⟩	67.3
DM + TnC	20.6	19.9 ± 0.07	12.7 ± 0.23	1.8
		21.1	⟨1⟩	69.7
		14.0	⟨25⟩	20.5
DM + POPC (no Ca^{2+})	21.2	21.0 ± 0.02	4.9 ± 0.14	2.6
		21.1	⟨1⟩	9.6
		14.0	⟨25⟩	155.1

[a] All solutions contained 5 mM Mops, pH 7, 20 °C, with 1 mM Ca^{2+}.
[b] The *hw* was held constant at the value inside the angular brackets.

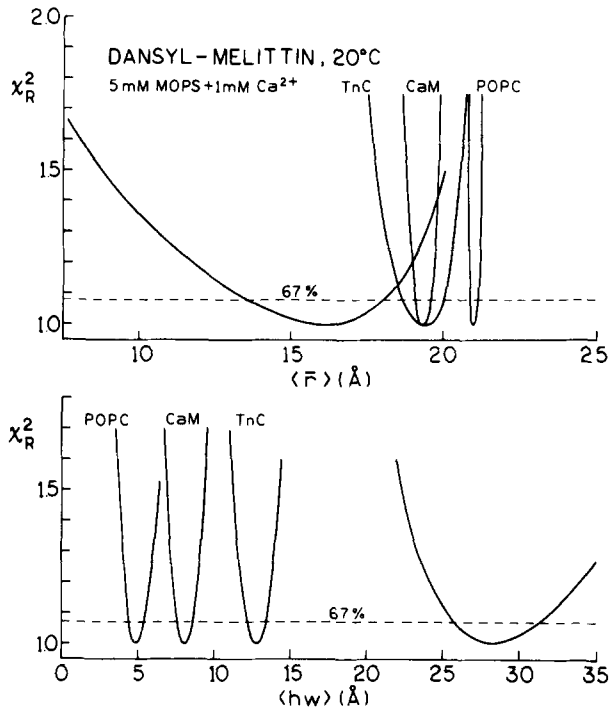

Fig. 9. χ_R^2 surfaces for the distance distribution $\bar{r}$ (top) and hw (bottom) of melittin and its complexes with CaM, TnC, or POPC, or in the random-coil state (5 mM MOPS + 1 mM Ca^{2+}).

$$P(r) = \begin{cases} \frac{1}{z}\exp\left[-\frac{1}{2}\left(\frac{r-\bar{r}}{\sigma}\right)^2\right] & \text{for } r_{min} \le r \le r_{max} \\ 0 & \text{elsewhere,} \end{cases} \quad (1)$$

where r_{min} and r_{max} are minimum and maximum donor–acceptor distances, Z is the normalization factor, $\bar{r}$ is the average, and σ is the SD of the distribution.

$$Z = \int_{r_{min}}^{r_{max}} \exp\left[-\frac{1}{2}\left(\frac{r-\bar{r}}{\sigma}\right)^2\right]. \quad (2)$$

The value σ is related to hw (full width at half maximum) by $hw = 2.355\sigma$. The use of a Gaussian is an approximation, which may be refined by further experimentation. The limited resolution of the data requires the assumption of a functional form for the distribution. We chose a Gaussian distribution because this is comparable to that expected from long alkyl chains (Flory, 1969), and other distributions such as a rectangular or Lorentzian distribution are unlikely for a flexible molecule.

For an infinite flexible chain all possible solid angles are available at each distance, and Equation 1 could be written to contain a factor of $4\pi r^2$ in the numerator to account for a 3-dimensional volume element (Flory, 1969). However, the selection of the volume element is not clear for donor and acceptor proteins, especially for a structured and/or globular protein for which the acceptor may be restricted to a limited range of solid angles relative to the donor. In the absence of specific knowledge of the volume element we used the simple Gaussian given by Equation 1, and we take $P(r)$ as indicating the probability of an acceptor being present with the distance r to $r + dr$, irrespective of the solid angle accessible to the acceptor. This formalism has the advantage of providing the distance-distribution results in an intuitive manner, in which $\bar{r}$ and hw values are easily related to the size and conformation of the protein.

The information necessary to recover $P(r)$ is contained in the intensity decay of the donor. More specifically, suppose the donor displays a single-exponential decay in the absence of acceptor. The presence of an acceptor over a range of distance results in a complex nonexponential decay of the donor. The distance-distribution information is provided by the extent of energy transfer quenching and the extent of nonexponentiality induced in the donor decay by the acceptor. In practice, the situation is somewhat more complex because the intensity decays of most proteins, even those containing a single Trp residue, are usually multiexponential (Grinvald & Steinberg, 1976; Beechem et al., 1985). Hence, recovery of the distance distributions requires measurement of the multiexponential donor decays, and then further measurements of the effects of the acceptor and a range of transfer rates on this decay.

The intensity decays of the Trp donor were recovered from the frequency response of its emission. In the frequency domain one measures the phase (ϕ_ω) and modulation (m_ω) of the emission over a range of modulation frequencies (ω). These data are fit to the multiexponential model

$$I_D(t) = \sum_i \alpha_{Di} \exp[-t/\tau_{Di}], \quad (3)$$

where α_{Di} is the preexponential factor and τ_{Di} the associated decay time. For Equation 3 or for any intensity decay law, the frequency response (ϕ_ω and m_ω) can be calculated using (Gratton et al., 1983; Lakowicz et al., 1985)

$$N_\omega = \int_0^\infty I_D(t)\sin \omega t\, dt \quad (4)$$

$$D_\omega = \int_0^\infty I_D(t)\cos \omega t\, dt \quad (5)$$

$$J = \int_0^\infty I_D(t)\, dt. \quad (6)$$

The calculated (c) phase and modulation values for the assumed decay law are given by

$$\phi_{c\omega} = \arctan\left[\frac{N_\omega}{D_\omega}\right] \quad (7)$$

$$m_{c\omega} = \frac{1}{J}[N_\omega^2 + D_\omega^2]^{1/2}. \quad (8)$$

The parameters describing the intensity decay (α_{Di} and τ_{Di}) are found using nonlinear least squares (Bevington, 1969) by varying α_{Di} and τ_{Di} to obtain the minimum value of χ_R^2:

$$\chi_R^2 = \frac{1}{\nu}\sum_\omega \left[\frac{\phi_\omega - \phi_{c\omega}}{\delta\phi}\right]^2 + \frac{1}{\nu}\sum_\omega \left[\frac{m_\omega - m_{c\omega}}{\delta m}\right]^2, \quad (9)$$

where ν is the number of degrees of freedom and $\delta\phi$ and δm are the experimental uncertainties in the measured phase and modulation values.

Somewhat more complex expressions are needed to calculate the frequency response in the presence of energy transfer and a distribution of donor–acceptor distances. Consider a single donor–acceptor pair separated by a distance r. We assume that the transfer rates for each component in the decay are given by the usual expression:

$$k_{DAi} = \frac{1}{\tau_{Di}}\left[\frac{R_0}{r}\right]^6, \tag{10}$$

where R_0 is the Förster distance (Förster, 1948) for energy transfer. The distance-dependent donor decay times are then given by

$$\frac{1}{\tau_{DAi}} = \frac{1}{\tau_{Di}} + \frac{1}{\tau_{Di}}\left[\frac{R_0}{r}\right]^6. \tag{11}$$

Under this assumption the intensity decay of a donor–acceptor pair spaced by a distance r is given by

$$I_{DA}(r, t) = \sum_i \alpha_{Di} \exp\left[-\frac{t}{\tau_{Di}} - \frac{t}{\tau_{Di}}\left(\frac{R_0}{r}\right)^6\right]. \tag{12}$$

In the actual experiment one does not observe a single donor–acceptor pair but rather observes an ensemble of donor–acceptor pairs weighted by their relative populations and probability of donor emission. Hence, the observed decay is given by

$$I_{DA}(t) = \int_{r_{min}}^{r_{max}} P(r) I_{DA}(r, t)\, dr. \tag{13}$$

The sine and cosine transforms are

$$N_\omega = \int_{r_{min}}^{r_{max}} P(r) \sum_i \frac{\alpha_{Di}\omega\tau_{DAi}^2}{1 + \omega^2\tau_{DAi}^2}\, dr \tag{14}$$

$$D_\omega = \int_{r_{min}}^{r_{max}} P(r) \sum_i \frac{\alpha_{Di}\tau_{DAi}}{1 + \omega^2\tau_{DAi}^2}\, dr, \tag{15}$$

where the normalization factor J is given by

$$J = \int_{r_{min}}^{r_{max}} P(r) \sum_i \alpha_{Di}\tau_{DAi}\, dr. \tag{16}$$

The parameters describing the distance distribution ($\bar{r}$ and hw) are recovered from least-squares analysis, as described for the multiexponential decay (Equation 9). It is important to note that a multiexponential decay for the donor does not introduce any additional parameters into the analysis. This is because the intrinsic decays of the donor are measured in a separate experiment, using samples without an acceptor. The data from the donor are fit using the multiexponential model, and the parameters (α_{Di} and τ_{Di}) are held constant in Equations 14–16 during the least-squares analysis. It should be remembered that τ_{DAi} depends on distance (Equation 11).

Estimation of the uncertainties in the recovered parameters is a difficult problem. We used 2 different methods, both of which resulted in similar estimated uncertainties. Our analysis programs calculate the uncertainties by examination of the range of parameter values that are consistent with the data (Johnson, 1983). We also estimate the uncertainty in a parameter value by adjusting its value to a slightly different value. This value is held fixed, and the other parameters are varied to once again minimize χ_R^2. Both these methods should account for correlation between the parameters, which allows the parameter values to vary in a concerted manner without significantly altering χ_R^2.

The Förster distance R_0 can be calculated from the spectral properties of the chromophores (Förster, 1948),

$$R_0^6 = \frac{9{,}000(\ln 10)\kappa^2\phi_D}{128\pi^5 N n^4}\int_0^\infty F_D(\lambda)\epsilon_A(\lambda)\lambda^4\, d\lambda, \tag{17}$$

where κ^2 is the orientation factor, ϕ_D is the quantum yield of the donor in the absence of the acceptor, n is the refractive index, N is Avogadro's number, $F_D(\lambda)$ is the emission spectrum of the donor with the area normalized to unity, $\epsilon_A(\lambda)$ is the absorption spectrum of the acceptor in units of M^{-1} cm^{-1}, and λ is the wavelength in nm. The distances obtained using the R_0 value are somewhat uncertain because of their dependence upon the extent of static and dynamic averaging of the orientation factor (Dale & Eisinger, 1975; Dale et al., 1979). In our analysis, we assume the value of κ^2 is equal to 2/3 due to the range of conformations, the possibility of rotational diffusion, and the mixed polarization of the species (Haas et al., 1978). It should be noted that the use of $\kappa^2 = 2/3$ is not likely to result in significant error if the donor and acceptor can adopt a range of conformations (Englert & Leclerc, 1978).

Steady-state measurements of the efficiency of energy transfer (E) have been widely used to measure discrete donor-to-acceptor distances. However, it should be noted that the steady-state data can only be used to calculate an apparent (R_{app}) donor-to-acceptor distance,

$$E = \frac{R_0^6}{R_0^6 + R_{app}^6}. \tag{18}$$

We used the anisotropy decays of melittin and its complexes to estimate their hydrodynamic volumes and the extent of donor and acceptor mobility. The anisotropy decays were obtained from the polarized frequency-domain data as described previously (Lakowicz et al., 1985, 1986a; Faucon & Lakowicz, 1987). The data were fit to an anisotropy decay law,

$$r(t) = \sum_j r_0 g_j e^{-t/\theta_j}, \tag{19}$$

where $r_0 g_j$ are the amplitudes associated with each correlation time θ_j. In this expression the fundamental anisotropy (r_0) can be taken as a known value, in which case $\sum g_j = 1.0$. Alternatively, if r_0 is not known, then the values of $r_0 g_j$ are each varied to minimize χ_R^2.

Materials and methods

Synthetic *N*-α-amino-dansylated melittin was prepared using standard procedures for solid-phase peptide synthesis (Weaver

et al., 1989), followed by purification by reverse-phase HPLC on a C_8 column. Melittin concentrations were determined from absorbance and the known extinction coefficient (Maulet & Cox, 1983) and were typically near 2×10^{-5} M. For dansyl-melittin, mass spectrometry (performed by Ian Jardines, Department of Pharmacology, Mayo Foundation, Rochester, Minnesota) showed a single species each with 1 dansyl moiety. The concentration of dansyl-melittin was also determined from absorbance values at 280 nm with the contribution of the dansyl at 280 nm added to the extinction due to the Trp side chain. Unless stated otherwise, all solutions were in 5 mM Mops, 1 mM Ca^{2+}, pH 7, 20 °C. Solutions containing POPC (1 mM) did not contain Ca^{2+}. Emission spectra were recorded for all samples and appropriate controls and did not reveal the presence of any significant fluorescent impurities Bovine CaM was HPLC purified and obtained from Professor Robert Steiner at the University of Maryland.

Frequency-domain measurements were performed on the instrument described previously (Lakowicz et al., 1986b). The excitation source was a 3.79-MHz train of pulses, about 7 ps wide, obtained from the cavity-dumped output of a synchronously pumped rhodamine 6G dye laser. The dye laser output was frequency-doubled to 295 nm. This source is intrinsically modulated to many GHz and is used directly to excite the sample. The modulated emission was detected using a microchannel plate photomultiplier tube, R1564U (Hamamatsu Corp.). All intensity decays were measured using rotation-free polarization conditions, with the donor emission selected by a 340-nm interference filter, 10-nm bandwidth. For all analyses the uncertainties in the phase ($\delta\phi$) and modulation (δm) values were taken as 0.2° and 0.005, respectively.

For calculation of R_0, the Trp quantum yields were measured by comparison with Trp in water, using a yield of 0.13 (Chen, 1967).

Acknowledgments

This work was supported by grant GM 35154 from the National Institutes of Health, with support for the Center for Fluorescence Spectroscopy from the National Science Foundation (DIR-8710401) and the National Institutes of Health (RR-08119). J.R.L. and G.L. thank the Medical Biotechnology Center, University of Maryland, for financial support. We thank Drs. Frank Prendergast, A.J. Weaver, and M.D. Kemple (Mayo Foundation, Rochester, Minnesota) for providing the labeled and unlabeled synthetic melittin, which was essential for this research.

References

Amir D, Haas E. 1986. Determination of intermolecular distance distributions in a globular protein by nonradiative excitation energy transfer measurements. *Biopolymers 25*:235–240.

Babu YS, Bugg CE, Cook WJ. 1988. Structure of calmodulin refined at 2.2 Å resolution. *J Mol Biol 204*:191–204.

Babu YS, Sack JS, Greenhough TJ, Bugg CE, Means AR, Cook WJ. 1985. Three-dimensional structure of calmodulin. *Nature 315*:37–42.

Bazzo R, Tappin MJ, Pastore A, Harvey TS, Carver JA, Campbell ID. 1988. The structure of melittin A ^{1}H-NMR study in methanol. *Eur J Biochem 173*:139–146.

Beals JM, Haas E, Krausz S, Scheraga HA. 1991. Conformational studies of a peptide corresponding to a region of the C-terminus of ribonuclease A: Implications as a potential chain-folding initiation site. *Biochemistry 30*:7680–7692.

Beechem JM, Ameloot M, Brand L. 1985. Global analysis of fluorescence decay surfaces: Excited state reactions. *Chem Phys Lett 120*:466–472.

Beschiaschvili G, Seelig J. 1990. Melittin binding to mixed phosphatidylglycerol/phosphatidylcholine membranes. *Biochemistry 29*:52–58.

Bevington PR. 1969. *Data reduction and error analysis for the physical sciences*. New York: McGraw-Hill Book Company.

Chen RF. 1967. Fluorescence quantum yields of tryptophan and tyrosine. *Anal Lett 1*:35–42.

Cheung HC. 1991. Resonance energy transfer. In: Lakowicz JR, ed. *Topics in fluorescence spectroscopy: Principles, vol 2*. New York: Plenum Press. pp 127–176.

Comte M, Maulet Y, Cox JA. 1983. Ca^{2+}-dependent high-affinity complex formation between calmodulin and melittin. *Biochem J 209*:269–272.

Dale RE, Eisinger J. 1975. Polarized excitation energy transfer. In: Chen RF, Edelhoch H, eds. *Biochemical fluorescence: Concepts*. New York: Marcel Dekker. pp 115–284.

Dale RE, Eisinger J, Blumberg WE. 1979. The orientation freedom of molecular probes. *Biophys J 26*:161–194.

Dawson CR, Drake AF, Helliwell J, Hider RC. 1978. The interaction of bee melittin with lipid bilayer membranes. *Biochim Biophys Acta 510*:75–86.

Dempsey C, Bitbol M, Watts A. 1989. Interaction of melittin and mixed phospholipid membranes composed of dimyristoylphosphatidylcholine and dimyristoylphosphatidylserine studied by deuterium NMR. *Biochemistry 28*:6590–6596.

Drake AF, Hider RC. 1979. The structure of melittin in lipid bilayer membranes. *Biochim Biophys Acta 555*:371–373.

Englert A, Leclerc M. 1978. Intramolecular energy transfer in molecules with a large number of conformations. *Proc Natl Acad Sci USA 75*:1050–1051.

Faucon JF, Dufourcq J, Lurson C. 1979. The self-association of melittin and its binding to lipids. *FEBS Lett 102*:187–190.

Faucon JF, Lakowicz JR. 1987. Anisotropy decay of DPH in melittin-phospholipid complexes by multi-frequency phase-modulation fluorometry. *Arch Biochem Biophys 245*:245–258.

Flory PJ. 1969. *Statistical mechanics of chain molecules*. New York: Interscience, John Wiley & Sons.

Follenius-Wund A, Hely Y, Gerard D. 1987. Spectroscopic evidence of two melittin molecules bound to Ca^{2+}-calmodulin. *Biochem Int 15*(4):823–833.

Förster T. 1948. Intermolecular energy migration and fluorescence. *Ann Phys (Leipzig) 2*:55–75.

Goto Y, Hagihara Y. 1992. Mechanism of the conformational transition of melittin. *Biochemistry 31*:732–738.

Gratton E, Limkeman M. 1983. A continuous variable-frequency cross-correlation phase fluorometer with picosecond resolution. *Biophys J 44*:315–324.

Gratton E, Limkeman M, Lakowicz JR, Maliwal BP, Cherek H, Laczko G. 1983. Resolution of mixtures of fluorophores using variable-frequency phase and modulation data. *Biophys J 46*:479–486.

Grinvald A, Steinberg IZ. 1976. The fluorescence decay of tryptophan residues in native and denatured proteins. *Biochim Biophys Acta 427*:663–678.

Haas E, Katchalski-Katzir E, Steinberg IZ. 1978. Effect of the orientation of donor and acceptor on the probability of energy transfer involving transitions of mixed polarization. *Biochemistry 17*:5064–5070.

Haas E, Wilchek H, Katchalski-Katzir E, Steinberg IZ. 1975. Distribution of end-to-end distances of oligopeptides in solution as estimated by energy transfer. *Proc Natl Acad Sci USA 72*:1807–1811.

Hedstrom JF, Prendergast FG, Miller LJ. 1990. Conformational analysis of peptides using time-resolved fluorescence resonance energy transfer. In: Rivier JE, Marshall GR, eds. *Peptides: Chemistry, structure and biology. Proceedings of the Eleventh American Peptide Symposium, La Jolla*. pp 651–652.

Heidorn DB, Seeger PA, Rokop SE, Blumenthal DK, Means AR, Crespi H, Trewhella J. 1989. Changes in the structure of calmodulin induced by a peptide based on the calmodulin-binding domain of myosin light chain kinase. *Biochemistry 28*:6757–6764.

Heidorn DB, Trewhella J. 1988. Comparison of the crystal and solution structure of calmodulin and troponin C. *Biochemistry 27*:909–915.

Herzberg O, James MNG. 1985. Structure of the calcium regulatory muscle protein troponin-C at 2.8 Å resolution. *Nature 313*:653–661.

Herzberg O, James MNG. 1988. Refined crystal structure of troponin-C from turkey muscle at 2.0 Å resolution. *J Mol Biol 203*:761–779.

Ikura M, Clore GM, Gronenborn AM, Zhu G, Klee CB, Bax A. 1992. Solution structure of a calmodulin-target peptide complex by multidimensional NMR. *Science 256*:632–638.

Johnson ML. 1983. Evaluation and propagation of confidence intervals in nonlinear, asymmetrical variance spaces. *Biophys J 44*:101–106.

Kaschke M, Valeur B, Bourson J, Ernsting NP. 1991. Recovery of the distribution of interchromophoric distances in a donor-acceptor coumarin supermolecule by time-resolved energy transfer measurements. *Chem Phys Lett 179*:544–550.

Knoppel E, Eisenberg D, Wickner W. 1979. Interactions of melittin, a preprotein model, with detergents. *Biochemistry 18*:4177–4181.

Kretsinger RH, Rudrick SE, Weissman LF. 1986. Crystal-structure of calmodulin. *F Inorg Biochem 28*:289–302.

Kuchina E, Seelig J. 1989. Interaction of melittin with phosphatidylcholine membranes. Binding isotherm and lipid head-group conformation. *Biochemistry 28*:4216–4221.

Lakowicz JR, Cherek H, Gryczynski I, Joshi N, Johnson ML. 1987a. Enhanced resolution of fluorescence anisotropy decays by simultaneous analysis of progressively quenched samples; applications to anisotropic rotations and protein dynamics. *Biophys J 51*:755–768.

Lakowicz JR, Cherek H, Maliwal BP, Gratton E. 1985. Time-resolved fluorescence anisotropies of fluorophores in solvents and lipid bilayers obtained from frequency-domain phase-modulation fluorometry. *Biochemistry 24*:376–383.

Lakowicz JR, Gryczynski I, Cherek H. 1986a. Measurement of subnanosecond anisotropy decays of protein fluorescence using frequency-domain fluorometry. *J Biol Chem 261*:2240–2245.

Lakowicz JR, Gryczynski I, Cheung HC, Wang C, Johnson ML. 1988a. Distance distributions in native and random-coil troponin I from frequency-domain measurements of fluorescence energy transfer. *Biopolymers 27*:821–830.

Lakowicz JR, Gryczynski I, Cheung HC, Wang C, Johnson ML, Joshi N. 1988b. Distance distributions in proteins recovered by using frequency-domain fluorometry. Applications to troponin I and its complex with troponin C. *Biochemistry 27*:9149–9160.

Lakowicz JR, Gryczynski I, Kuśba J, Wiczk W, Szmacinski H, Johnson ML. 1994. Site-to-site diffusion in proteins as observed by energy transfer and frequency-domain fluorometry. *Photochem Photobiol 59*:16–29.

Lakowicz JR, Johnson ML, Wiczk W, Bhat A, Steiner RF. 1987b. Resolution of a distribution of distances by fluorescence energy transfer and frequency-domain fluorometry. *Chem Phys Lett 138*:587–593.

Lakowicz JR, Laczko G, Gryczynski I. 1986b. A 2 GHz frequency-domain fluorometer. *Rev Sci Instrum 57*:2499–2506.

Lakowicz JR, Maliwal BP. 1985. Construction and performance of a variable-frequency phase-modulation fluorometer. *Biophys Chem 21*: 61–78.

Lakowicz JR, Wiczk W, Laczko G, Prendergast FG, Johnson ML. 1990. Conformational distributions of melittin in water/methanol mixtures from frequency-domain measurements of non-radiative energy transfer. *Biophys Chem 36*:99–115.

Lavialle F, Adams RG, Levin IW. 1982. Infrared spectroscopic study of the secondary structure of melittin in water, 2-chloroethanol, and phospholipid bilayer dispersions. *Biochemistry 21*:2305–2312.

Maulet Y, Cox JA. 1983. Structural changes in melittin and calmodulin upon complex formation and their modulation by calcium. *Biochemistry 22*: 5681–5686.

Meador WE, Means AR, Quiocho FA. 1992. Target enzyme recognition by calmodulin: 2.4 Å structure of a calmodulin–peptide complex. *Science 257*:1251–1255.

Meador WE, Means AR, Quiocho FA. 1993. Modulation of calmodulin plasticity in molecular recognition on the basis of X-ray structure. *Science 262*:1718–1721.

Milos M, Schaer JJ, Comte M, Cox JA. 1987. Microcalorimetric investigation of the interactions in the ternary complex calmodulin–calcium–melittin. *J Biol Chem 262*(6):2746–2749.

Precheur B, Munier H, Mispelter J, Barzu O, Craescu CT. 1992. ^{1}H and ^{15}N NMR characterization of free and bound states of an amphophilic peptide interacting with calmodulin. *Biochemistry 31*:229–236.

Prochazka K, Kiserow D, Ramireddy C, Tuzar Z, Munk P, Webber SE. 1992. Time-resolved fluorescence studies of the chain dynamics of naphthalene-labeled polystyrene-block-poly(methacrylic acid). *Macromolecules 25*: 454–460.

Roth SM, Schneider DM, Strobel LA, VanBerkum MFA, Means AR, Wand J. 1991. Structure of the smooth muscle myosin light-chain kinase calmodulin-binding domain peptide bound to calmodulin. *Biochemistry 30*:10078–10084.

Satyshur KA, Rao ST, Pysalska D, Drendel W, Greaser M, Sundaralingam M. 1988. Refined structure of chicken skeletal muscle troponin C in the two-calcium state at 2 Å resolution. *J Biol Chem 263*:1628–1647.

Stanislawski B, Rüterjans H. 1987. ^{13}C-NMR investigation of the insertion of the bee venom melittin into lecithin vesicles. *Eur Biophys J 15*:1–12.

Steiner RF. 1991. Fluorescence anisotropy: Theory and applications. In: Lakowicz JR, ed. *Topics in fluorescence spectroscopy: Principles, vol 2*. New York: Plenum Press. pp 1–52.

Steiner RF, Marshall L, Needleman D. 1986. The interaction of melittin and its tryptic fragments. *Arch Biochem Biophys 246*:286–300.

Steiner RF, Norris L. 1987. The interaction of melittin with troponin C. *Arch Biochem Biophys 254*:342–352.

Strom R, Crifo C, Viti V, Guidoni L, Podo F. 1978. Variations in circular dichroism and proton-NMR relaxation properties of melittin upon interaction properties of melittin upon interaction with phospholipids. *FEBS Lett 96*:45–50.

Stryer L, Haugland RP. 1967. Energy transfer: A spectroscopic ruler. *Proc Natl Acad Sci USA 58*:719–726.

Strynadka NCJ, James MNG. 1990. Model for the interaction of amphophilic helices with troponin C and calmodulin. *Proteins Struct Funct Genet 7*:234–218.

Sundaralingam M, Bergstrom R, Strasburg G, Greaser M, Wang BC. 1985. Molecular structure of troponin C from chicken skeletal muscle at 3-Ångstrom resolution. *Science 227*:945–948.

Talbot JC, Dufourcq J, DeBong J, Faucon JF, Lurson C. 1979. Conformational change and self-association of monomeric melittin. *FEBS Lett 102*:191–193.

Terwilliger TC, Eisenberg D. 1982. The structure of melittin. II. Interpretation of the structure. *J Biol Chem 257*:6016–6022.

Terwilliger TC, Weissman L, Eisenberg D. 1982. The structure of melittin in the form I crystals and its implication for melittin's lytic and surface activities. *Biophys J 37*:353–361.

Vorherr T, Kessler O, Mark A, Carafoli E. 1992. Construction and molecular dynamics simulation of calmodulin in the extended and in a bent conformation. *Eur J Biochem 204*:931–937.

Weaver AJ, Kemple MD, Prendergast FG. 1989. Characterization of selectively ^{13}C-labeled synthetic melittin and melittin analogues in isotropic solvents by circular dichroism, fluorescence, and NMR spectroscopy. *Biochemistry 28*:8614–8623.